NEURAL REGENERATION RESEARCH
www.nrronline.org

Research Article

Vav1 promotes inflammation and neuronal apoptosis in cerebral ischemia/reperfusion injury by upregulating microglial and NLRP3 inflammasome activation

Jing Qiu[1, #], Jun Guo[2, #], Liang Liu[1], Xin Liu[1], Xianhui Sun[1], Huisheng Chen[1, *]

https://doi.org/10.4103/1673-5374.371368

Date of submission: August 24, 2022

Date of decision: January 16, 2023

Date of acceptance: February 14, 2023

Date of web publication: March 15, 2023

From the Contents

Graphical Abstract

Vav1, affecting microglial and NLRP3 inflammasome activation, aggravates cerebral I/R injury caused inflammation and neuronal apoptosis

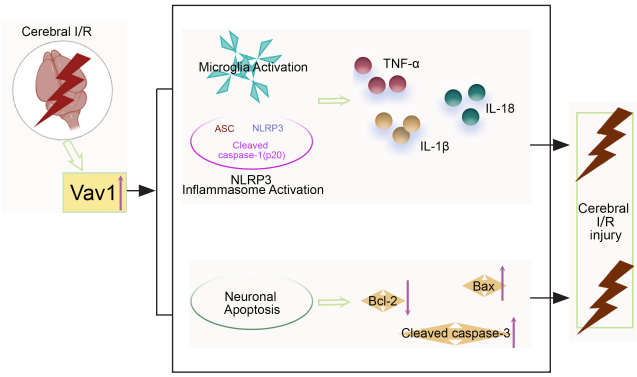

Abstract

Microglia, which are the resident macrophages of the central nervous system, are an important part of the inflammatory response that occurs after cerebral ischemia. Vav guanine nucleotide exchange factor 1 (*Vav1*) is a guanine nucleotide exchange factor that is related to microglial activation. However, how *Vav1* participates in the inflammatory response after cerebral ischemia/reperfusion injury remains unclear. In this study, we subjected rats to occlusion and reperfusion of the middle cerebral artery and subjected the BV-2 microglia cell line to oxygen-glucose deprivation/reoxygenation to mimic cerebral ischemia/reperfusion *in vivo* and *in vitro*, respectively. We found that Vav1 levels were increased in the brain tissue of rats subjected to occlusion and reperfusion of the middle cerebral artery and in BV-2 cells subjected to oxygen-glucose deprivation/reoxygenation. Silencing *Vav1* reduced the cerebral infarct volume and brain water content, inhibited neuronal loss and apoptosis in the ischemic penumbra, and improved neurological function in rats subjected to occlusion and reperfusion of the middle cerebral artery. Further analysis showed that Vav1 was almost exclusively localized to microglia and that *Vav1* downregulation inhibited microglial activation and the NOD-like receptor pyrin 3 (NLRP3) inflammasome in the ischemic penumbra, as well as the expression of inflammatory factors. In addition, *Vav1* knockdown decreased the inflammatory response exhibited by BV-2 cells after oxygen-glucose deprivation/reoxygenation. Taken together, these findings show that silencing *Vav1* attenuates inflammation and neuronal apoptosis in rats subjected to cerebral ischemia/reperfusion through inhibiting the activation of microglia and NLRP3 inflammasome.

Key Words: apoptosis; cerebral ischemia/reperfusion; inflammatory cytokines; microglia; microglial activation; middle cerebral artery occlusion; neuroprotection; NLRP3 inflammasome; oxygen-glucose deprivation/reoxygenation; *Vav1*

Introduction

Cerebrovascular diseases caused by ischemia have been identified as a major cause of human mortality (Campbell et al., 2019; Stegner et al., 2019; Zeng et al., 2022). Once ischemia occurs, the brain rapidly undergoes pathological changes and suffers irreversible damage (Øie et al., 2020; Wang et al., 2020b). Reperfusion, which restores blood flow and delivers oxygen to the ischemic brain, is a common strategy for the treatment of cerebral ischemia (Chandra et al., 2017). Unfortunately, this process inevitably leads to greater cell death and tissue damage, which is also known as cerebral ischemia/reperfusion (I/R) injury (Kalogeris et al., 2012; Bavarsad et al., 2019). Several studies have investigated the mechanism of cerebral I/R injury (Sun et al., 2003; Marlier et al., 2015). The currently accepted model of cerebral I/R pathogenesis includes inflammation, oxidative stress, apoptosis, and necrosis (Moskowitz et al., 2010). The inflammation that occurs after cerebral ischemia is a particularly critical factor in cerebral I/R injury (Lambertsen et al., 2012). Microglia, which are the resident macrophages of the central nervous system, are rapidly activated after ischemia, thus participating in the inflammatory response (Takeda et al., 2021). In addition, microglia can produce pro-inflammatory factors, reactive oxygen species, nitric oxide, and other factors that are important determinants of neuronal death in cerebral ischemia (Tan et al., 2021). Accordingly, inhibiting microglial activation may be the key to promoting neuronal parenchyma resistance to cerebral ischemia (Surinkaew et al., 2018).

Vav guanine nucleotide exchange factor 1 (*Vav1*, also known as *Vav*) was the first member of the *Vav* family to be identified (Katzav et al., 1989; Henske et al., 1995; Movilla and Bustelo, 1999). *Vav1* plays a key role in hematopoietic cell activation, growth, and differentiation (Turner and Billadeau, 2002; Hong et al., 2020). In Alzheimer's disease, *miR326* reduces neuronal apoptosis by downregulating *Vav1* expression (He et al., 2020). In addition, a previous study showed that *Vav1* may function as a downstream effector of *Nur77* to promote microglial activation (Chen et al., 2017). Shah and coworkers (Shah et al., 2009) also showed that *Vav1* is required for phosphatidylinositol3-kinase (PI3K) activation and demonstrated elevated *Vav1* levels in microglia stimulated with β-glucan. *PI3K* has been shown to activate the NOD-like receptor pyrin 3 (NLRP3) inflammasome (Kim et al., 2020). In addition, Inoue and coworkers (Inoue et al., 2012) found that *Vav1* acts as an upstream signaling molecule in NLRP3 inflammasome activation. Evidence also shows that microglia promote the release of inflammatory factors by activating the NLRP3 inflammasome (Ji et al., 2017). Taken together, these studies suggest

[1]Department of Neurology, General Hospital of Northern Theater Command, Shenyang, Liaoning Province, China; [2]Department of Neurology, Tangdu Hospital, Air Force Medical University, Xi'an, Shaanxi Province, China

***Correspondence to:** Huisheng Chen, PhD, chszh@aliyun.com.

https://orcid.org/0000-0002-7486-1992 (Huisheng Chen)

#Both authors contributed equally to this work.

Funding: *This study was supported by the Natural Science Foundation of Liaoning Province (General Program), No. 2017010825 (to JQ).*

How to cite this article: *Qiu J, Guo J, Liu L, Liu X, Sun X, Chen H (2023) Vav1 promotes inflammation and neuronal apoptosis in cerebral ischemia/reperfusion injury by upregulating microglial and NLRP3 inflammasome activation. Neural Regen Res 18(11):2436-2442.*

that *Vav1* may be closely related to inflammation and neuronal apoptosis. Importantly, using database analysis we found that *Vav1* is highly expressed in rats that have experienced cerebral I/R injury. Accordingly, we hypothesized that the high *Vav1* level displayed in cerebral I/R injury may promote microglial and NLRP3 inflammasome activation. In this study, we aimed to explore the role that *Vav1* plays in cerebral I/R-induced inflammation and neuronal apoptosis.

Methods

Database analysis

The Gene Expression Omnibus (GEO) database GSE163614 (https://www.ncbi.nlm.nih.gov/geo/query/acc.cgi?acc=GSE163614) (Yi et al., 2021) was used to explore *Vav1* expression levels in sham and cerebral I/R-injured rats.

Animals

The animal experiments were approved by the Animal Medical Research Ethics Committee of the General Hospital of the Northern Theater Command (approval No. 2022-04) on March 21, 2022. The animal experiments were conducted in accordance with Animal Research: Reporting of *In Vivo* Experiments (ARRIVE) guidelines (Percie du Sert et al., 2020). Male Sprague-Dawley rats (specific pathogen-free level, 8–10 weeks old, weighing 260–300 g, Huafukang Biotech, Beijing, China, license No. SCXK (Jing) 2019-0008) were used in the *in vivo* study. Rats were housed in a temperature-controlled room (temperature 22 ± 1°C, humidity 45–55%) with a 12/12-hour light/dark cycle and allowed *ad libitum* access to food and water for 1 week.

For the first part of the study, rats were randomly divided into two groups: sham (n = 12) and middle cerebral artery occlusion/reperfusion (MCAO/R) (n = 12). For the second part of the study, rats were randomly divided into four groups: sham (n = 24), MCAO/R (n = 24), MCAO/R + siNC (n = 24), and MCAO/R + *siVav1* (n = 24).

Middle cerebral artery occlusion/reperfusion model and small interfering RNA treatment

Twenty-four hours before MCAO was induced, rats were anesthetized by isoflurane (Shenzhen Ruiwode Life Technology Co. Ltd., Shenzhen, China, R510-22-10) inhalation, induced at 2.0% and maintained at 2.5%. The *Vav1* small interfering RNA and its negative control (General Biotech, Chuzhou, China) were administered by intra-cerebroventricular injection into the left lateral cerebral ventricle. The specific location for injection was as follows: 1.0 mm posterior to the bregma, 2.0 mm from the midline, and 3.5 mm beneath the skull surface (Wang et al., 2020c). A previously described suture occlusion method (Wu et al., 2018; Wang et al., 2020a) was used, with minor modifications. First, an incision was made in neck, and the right common carotid artery, internal carotid artery, and external carotid artery were isolated. The external carotid artery and its bifurcation were ligated with nylon suture, and the proximal external carotid artery, common carotid artery, and the distal end of the internal carotid artery were clipped with a clamp. A small cut was made at the bifurcation of the external carotid artery using a piece of ophthalmic scissors. The occlusion sutures were inserted into the head and the clamp at the distal end of the internal carotid artery was loosened. The round end of the nylon suture was then gradually inserted into the internal carotid artery, passing through the origin of the anterior cerebral artery, and blocking the middle cerebral artery. The incision was subsequently closed, leaving a 1-cm nylon suture to facilitate reperfusion (Longa et al., 1989). After 1.5 hours, the sutures were removed to allow reperfusion (He et al., 2015). The sham rats underwent the same surgery without MCAO. After 24 hours, the rats were sacrificed for further investigation. The ischemic penumbra of rat brain tissues was applied for further detection.

Cell culture and transfection

The mouse microglia cell line BV-2 (iCELL, Shanghai, China, Cat# iCell-m011, RRID: CVCL_0182) was used as an *in vitro* subject to further confirm the effect of *Vav1* on microglial and NLRP3 inflammasome activation. The cells were cultured in Dulbecco's modified Eagle medium (DMEM; Service Biotech, Wuhan, China, G4510) supplemented with 10% fetal calf serum (Tianhang Biotech, Zhejiang, China, 11011-8611). The cells were authenticated by short tandem repeat profiling and were checked for contamination using the ICLAC Database of Cross-contaminated or Misidentified Cell Lines.

The cells were maintained at 37°C with 5% CO_2 in a humidified incubator (Lishen Scientific Instrument Co., Ltd., Shanghai, China, HF-90). To induce oxygen-glucose deprivation/reoxygenation (OGD/R), the BV-2 cells were transferred to glucose-free Dulbecco's modified Eagle medium (Procell, Wuhan, China, PM150270) and placed in an incubator with a 5% CO_2, 94% N_2, and 1% O_2 atmosphere for 3 hours. Then, the cells were moved to an incubator with a 5% CO_2 atmosphere for another 21 hours. Lipofectamine 3000 (Invitrogen, 3000015) was used to carry out *Vav1* knockdown (75 pmol/well *Vav1* small interfering RNA) according to the manufacturer's instructions.

Quantitative polymerase chain reaction

Total RNA was extracted from the ischemic penumbra or from BV-2 cells using TRIpure lysis buffer (RP1001, BioTeke, Beijing, China) for 5 minutes. The concentration of the extracted RNA was determined by ultraviolet spectrophotometer (Nano2000, ThermoFisher, Waltham, MA, USA). Then, complementary DNA was synthesized using BeyoRT II M-MLV reverse transcriptase (D7160L, Beyotime, Shanghai, China). Subsequently, quantitative polymerase chain reaction (qPCR) was performed using SYBR Green (SY1020, Solarbio, Shanghai, China) and 2× Taq PCR MasterMix (PC1150, Solarbio) with an Exicycler TM96 real-time PCR system (BIONEER, Daejeon, Korea). The $2^{-\Delta\Delta Ct}$ method (Livak and Schmittgen, 2001) was used to determine the relative *Vav1* expression that normalized to *β-Actin*. The primer sequences were as follows: rat *Vav1*: 5′-CCA TTG CCC AGA ACA AA-3′ (forward, F), 5′-TCT CCA CGC AGT CAT AAA G-3′ (reverse, R); rat interleukin 1β (*IL-1β*): 5′-TGT GAT GTT CCC ATT AGA C-3′ (F), 5′-AAT ACC ACT TGT TGG CTT A-3′ (R); rat tumor necrosis factor (*TNF-α*): 5′-CCA CGC TCT TCT GTC TAC TG-3′ (F), 5′-GCT ACG GGC TTG TCA CTC-3′ (R); rat interleukin 18 (*IL-18*): 5′-GCC ATA CCA GAA GAA GG-3′ (F), 5′-TAG GGT CAC AGC CAG TC-3′ (R); Mus *Vav1*: 5′-GCT GAG CAC AAC TGG TGG GA-3′ (F), 5′-TGG CGA ACT CCG CTG TAT CT-3′ (R); Mus *IL-1β*: 5′-CTC AAC TGT GAA ATG CCA CC-3′ (F), 5′-GAG TGA TAC TGC CTG CCT GA-3′ (R); Mus *TNF-α*: 5′-CAG GCG GTG CCT ATG TCT CA-3′ (F), 5′-GCT CCT CCA CTT GGT GGT TT-3′ (R); Mus *IL-18*: 5′-GGC TGC CAT GTC AGA AGA-3′ (F), 5′-CCG TAT TAC TGC GGT TGT-3′ (R).

Western blot analysis

Proteins were extracted from the ischemic penumbra or from BV-2 cells using lysis buffer (Beyotime, P0013). A bicinchoninic acid (BCA) protein assay kit (Beyotime, P0011) was used to determine the concentration of the extracted proteins. Sodium dodecyl sulfate polyacrylamide gel electrophoresis (Beyotime, P0015) was used to separate samples, which were then electrophoretically transferred to polyvinylidene fluoride membranes (IPVH00010, Millipore, Billerica, MA, USA). Skim milk powder dissolved in Tris buffered saline with Tween 20 (5%, YiLi, Beijing, China) was used as the blocking buffer. After overnight incubation (4°C) with a primary antibody, the membranes were incubated with a goat anti-rabbit antibody (1:10,000, ABclonal, Wuhan, China, Cat# AS014, RRID: AB_2769854) for 40 minutes at 37°C. Finally, the signals were detected using an enhanced chemiluminescence reagent (Beyotime, P0018) according to the manufacturer's instructions. The results were analyzed using Tanon Image software (5200, Tanon Science & Technology Co, Beijing, China). The primary antibodies used were as follows: Vav1 (rabbit, 1:1000, Affinity Biosciences, Liyang, China, Cat# AF6182, RRID: AB_2835065), NLRP3 (rabbit, 1:1000, Abclonal, Cat# A5652, RRID: AB_2766412), Bcl-2 (rabbit, 1:1000, Abclonal, Cat# A19693, RRID: AB_2862738), apoptosis-associated speck-like protein containing CARD (ASC; rabbit, 1:1000, Abclonal, Cat# A16672, RRID: AB_2771891), Bax (rabbit, 1:150, Abclonal, Cat# A19684, RRID: AB_2862733), cleaved caspase-3 (rabbit, 1:150, Affinity Biosciences, Cat# AF7022, RRID: AB_2835326), and cleaved caspase-1 (rabbit, 1:150, Affinity Biosciences, Cat# AF4005, RRID: AB_2845463).

Triphenyltetrazolium chloride staining

The rats were sacrificed, and the brains were removed and stored at –20°C for 20 minutes. Then, the brain was cut longitudinally into five pieces. Triphenyltetrazolium chloride (TTC) staining solution (2 mL, 1%, Solarbio, Beijing, China, T8170) was added, and the brain slices were incubated at 37°C for 15 minutes in the dark. The stained slices were then photographed with a mobile phone, and the infarct area was calculated by determining the percentage of infarct area out of total brain tissue area in the five slices.

Neurological deficit score

Twenty-four hours after MCAO/R, the rats were scored based on the Zea-Longa neurological deficit score (Longa et al., 1989). The rats were scored as follows: 0: no deficiency; 1: unable to fully extend the contralateral claw; 2: circle to the contralateral side while walking; 3: lean to the injured side; and 4: unable to walk spontaneously and lose consciousness.

Brain water content

The rats were sacrificed, and the brains were removed, rinsed with normal saline, and dried with filter paper. Each brain was then weighed to determine the wet weight. Then, the brains were dried in a 100°C oven overnight and weighed to determine the dry weight. The brain water content (percentage) was calculated as follows: (wet weight – dry weight)/wet weight × 100.

Hematoxylin and eosin staining

The rats were sacrificed, the brains were removed, and the ischemic penumbras were fixed, dehydrated, and permeabilized in a decreasing alcohol and xylene gradient (1330-20-7, Aladdin, Shanghai, China). The sections were then treated with various concentrations of ethanol (Sinopharm Chemical Reagent, Beijing, China 10009218, China) and distilled water, followed by staining with hematoxylin (5 minutes, Solarbio, H8070) and eosin (3 minutes, Sangon, Shanghai, China, A600190). The stained sections were observed using a fluorescence microscope (BX53, Olympus, Tokyo, Japan).

Fluoro-Jade C staining

A Fluoro-Jade C (FJC) kit (Solarbio, G3263) was used to stain degenerating neurons according to the manufacturer's instructions. Brain sections (5 μm) containing the ischemic penumbra were isolated and prepared as described above. Next, the sections were placed in KMnO4 for 10 minutes. Then, the staining solution was added, and the sections were allowed to stain for 20 minutes in the dark. Images were obtained using a fluorescence microscope.

Immunofluorescence staining

Brain sections (5 μm) containing the ischemic penumbra were prepared as described above, and then soaked in xylene for 15 minutes followed by a graded alcohol series (95%, 85% and 75%) for 1 minute at each concentration. After antigen retrieval, 1% bovine serum albumin (Sangon, A602440-0050) was added as a blocking buffer, and the section were incubated at room temperature (20–30°C) for 15 minutes. Next, the cells were treated with 4% paraformaldehyde (Sinopharm Chemical Reagent, 80096618) and Triton X-100 (Beyotime, ST795) before blocking with 1% bovine serum albumin.

The sections were incubated with primary antibodies overnight at 4°C and with secondary antibodies for 1.5 hours at room temperature (20–30°C). DAPI (4′,6-diamidino-2′-phenylindole, Aladdin, D106471) was used to stain the nuclei. Then, an anti-fluorescence quenching agent (Solarbio, S2100) was added, and the sections were observed using a fluorescence microscope. The antibodies used were as follows: NLRP3 (rabbit, 1:200, Abclonal, Cat# A5652, RRID: AB_2766412), Vav1 (rabbit, 1:200, Proteintech, Wuhan, China, Cat# 16364-1-AP, RRID: AB_2213571), Iba-1 (mouse, 1:100, Abcam, Cambridge, UK, Cat# ab283319, RRID: AB_2924797), fluorescein isothiocyanate (FITC)-labeled goat anti-rabbit IgG (1:200, Abcam, Cat# ab6717, RRID: AB_955238), and Cy3-labeled goat anti-mouse IgG (1:200, Molecular Probes, Carlsbad, CA, USA, Cat# A-21424, RRID: AB_141780).

Cell apoptosis

Brain sections (5 μm) containing the ischemic penumbra were prepared as described above, and cell apoptosis was observed by immunofluorescence staining. A cell death detection kit (Roche, Basel, Switzerland, 12156792910) and a terminal-deoxynucleotidyl transferase mediated nick end labeling (TUNEL) kit (Wanleibio, Shenyang, China, WLA127a) were used according to the manufacturers' instructions. The brain sections were permeabilized with Triton X-100 (0.1%, 50 μL). After antigen retrieval, 50 μL TUNEL working buffer was added, and the sections were incubated in the dark at 37°C for 1 hour. Bovine serum albumin was used as the blocking buffer. Immunofluorescence staining was performed as described above with an anti-neuronal nuclear (NeuN) antibody (1:200, Abcam, ab104224) and FITC-labeled goat anti-mouse IgG (1:200, Abcam, ab6785).

Enzyme-linked immunosorbent assay

After sacrifice, the brain tissues contained ischemic penumbras were removed, weighted, and diluted ninefold in normal saline, followed by mechanical homogenization (ice) and centrifugation. A BCA kit (Solarbio, PC0020) was used to determine the protein concentration in each sample. BV-2 cell culture supernatant was collected by centrifugation. IL-1β content in the cell and brain samples was separately tested by the mouse (EK201B) and rat (EK301B) enzyme-linked immunosorbent assay (ELISA) kit (Multi Sciences, Hangzhou, China). TNF-α content in the cell and brain samples was determined using mouse (EK282) and rat (EK382) ELISA kits (Multi Sciences), respectively. IL-18 content in the cell and brain samples was determined using mouse (EK218, Multi Sciences) and rat (ER0030, Fine Test, Wuhan, China) ELISA kits, respectively. All ELISA assays were performed according to the manufacturers' instruction. The results were read using a microplate reader ELX-800 from BIOTEK (Winooski, VT, USA).

Statistical analysis

No statistical methods were used to predetermine the sample sizes; however, our sample sizes are similar to those reported in previous publications (Sun et al., 2020; Li et al., 2022). Six eligible rats were included in each group to ensure the accuracy and completeness of the experimental results. All evaluators were blinded to the assignments. Data were collected from independent experiments and are shown as means ± standard deviation (SD). One-way analysis of variance followed by Tukey's multiple comparisons test and unpaired *t*-test were performed using GraphPad Prism (version 8.0.0 for Windows, GraphPad Software, San Diego, CA, USA, www.graphpad.com). A significant difference was defined as a *P* value of less than 0.05.

Results

Increased *Vav1* expression in the ischemic penumbra of the MCAO/R rats

First, we explored *Vav1* expression in MCAO/R rats using a publicly available GEO database (GSE163614) and found that *Vav1* is highly expressed in MCAO/R rats (**Figure 1A**). On the basis of this, we examined *Vav1* mRNA and protein levels in the ischemic penumbra of MCAO/R rats. *Vav1* expression was significantly increased at both the mRNA (**Figure 1B**) and the protein (**Figure 1C**) level in MCAO/R rats compared with sham rats. Next, we used TTC staining to measure the cerebral infarction area of the MCAO/R rats and found a clear trend toward an increased percentage of infarction area in MCAO/R rats compared with sham rats (**Figure 1D**). These findings indicate that the enhancement of *Vav1* expression may play an important role in MCAO/R rats.

***Vav1* knockdown abates brain infarction and neuronal injury in MCAO/R rats**

Next, we inhibited *Vav1* expression in MCAO/R rats to explore the effect of Vav1 on brain infarction and neuronal injury after cerebral I/R. While Vav1 mRNA (**Figure 2A**) and protein (**Figure 2B**) expression levels were significantly increased in MCAO/R rats compared with sham rats, this effect was reversed by inhibition of *Vav1*. Then, we examined the cerebral infarction area in rat brain tissues by TTC staining. The images (**Figure 2C**) and quantitative results (**Figure 2D**) clearly showed that the infarction area in the MCAO/R rats was larger than that in sham rats, and this difference was strikingly decreased by *Vav1* knockdown. In addition, inhibiting *Vav1* expression ameliorated the neurological deficits seen in MCAO/R rats, as determined by neurological deficiency scoring (**Figure 2E**). When we assessed the brain water content, we found that it was higher in MCAO/R rats than in sham rats, and that inhibition of *Vav1* dramatically reversed this effect (**Figure 2F**). Finally, hematoxylin and eosin staining was used to analyze tissue damage in the ischemic penumbra of MCAO/R rats. Compared with the sham group, rats in the MCAO/R group showed aggravated damage in the ischemic penumbra, but inhibition of *Vav1* expression decreased this damage (**Figure 2G**). Taken together, these findings indicate that *Vav1* knockdown decreases brain infarction and neuronal injury in MCAO/R rats.

***Vav1* knockdown alleviates neuronal apoptosis in the ischemic penumbra of MCAO/R rats**

Cerebral I/R injury often results in neuronal degeneration and death (Xu et al., 2007; Liang et al., 2008), and therefore we used FJC and immunofluorescence staining to explore the role of *Vav1* in neuronal loss and apoptosis. Very little FJC staining was seen in sham rats, while FJC-positive neurons were clearly visible in MCAO/R rats (**Figure 3A** and **B**). However, *Vav1* inhibition clearly decreased the number of FJC-positive cells in MCAO/R rats compared with the negative control.

Next, we explored the effect of *Vav1* on neuronal apoptosis. Immunofluorescence staining for NeuN, a neuronal marker (Lavezzi et al., 2013), and TUNEL staining were used to detect neuronal apoptosis in the ischemic penumbra. MCAO/R resulted in a clear increase in the number of TUNEL-positive cells compared with sham rats (**Figure 3C** and **D**). However, *Vav1* knockdown decreased the number of TUNEL-positive cells in MCAO/R rats compared with the negative control. We also measured the expression of several intrinsic apoptotic markers, including Bcl-2, Bax, and cleaved caspase-3 (**Figure 3E** and **F**). Inhibition of *Vav1* significantly reversed the changes in the expression level of Bcl-2, Bax and cleavage of caspase-3, which was induced by MCAO/R. These results suggested that inhibiting *Vav1* expression decreases neuronal apoptosis in the brains of MCAO/R rats.

***Vav1* knockdown represses the inflammatory response in the ischemic penumbra of MCAO/R rats**

Inflammation after cerebral ischemia is an important factor leading to cerebral I/R injury (Li et al., 2021). As the resident macrophages of the central nervous system, microglia are involved in the inflammatory response to I/R (Wang et al., 2022). To determine whether microglia and the inflammasome were activated by MCAO/R in our rat model, we assessed expression of the microglial markers Iba-1 and Vav1, as well as NLRP3, an integral component of the inflammasome. The numbers of Iba-1/Vav1 double positive cells were increased in MCAO/R rats compared with sham rats, and inhibiting *Vav1* decreased this effect (**Figure 4A** and **B**). Merged images showed that Iba-1 and Vav1 co-localized more extensively in MCAO/R rats than in sham rats. The number of NLRP3-positive cells was higher in MCAO/R rats than in sham rats, while Vav1 inhibition reversed this effect (**Figure 4C** and **D**). Furthermore, as seen in **Figure 4C**, there was substantial co-localization of Iba-1 and NLRP3 in MCAO/R rats.

The NLRP3 inflammasome is composed of the sensor protein NLRP3, the adapter protein ASC, and the protease caspase-1 (Zangiabadi and Abdul-Sater, 2022). Therefore, we also examined the expression of these proteins. The western blot results (**Figure 5A** and **B**) showed that, compared with sham rats, NLRP3, ASC, and cleaved caspase-1 were expressed at significantly higher levels in MCAO/R rats. Similar to the effects shown in **Figure 4C**, this increase in protein expression was reversed by inhibition of *Vav1*. Furthermore, the mRNA and protein levels of IL-1β, TNF-α and IL-18 were enhanced after cerebral I/R, and this increase was abolished by inhibition of *Vav1* (**Figure 5C** and **D**). These results suggest that *Vav1* is involves in the inflammatory response in MCAO/R rats by affecting the activation of microglial and NLRP3 inflammasomes.

Increased *Vav1* expression in BV-2 cells subjected to OGD/R

Next, we constructed an OGD/R cell model in mouse BV-2 microglia cells to evaluate the effects of *Vav1 in vitro*. First, we assessed *Vav1* mRNA and protein levels in the cells. Consistent with the results from the *in vivo* experiments, *Vav1* expression was increased in BV-2 cells after OGD/R compared with the control cells (**Figure 6A** and **B**). Immunofluorescence staining confirmed that there were more Vav1-positive cells in the OGD/R group than in the control group (**Figure 6C** and **D**). Then, *Vav1* was silenced for further investigation (**Figure 6E** and **F**).

***Vav1* knockdown represses inflammation in BV-2 cells subjected to OGD/R**

The mRNA levels and contents of the *IL-1β*, *TNF-α*, and *IL-18* were also detected *in vitro*. Compared with the control, *IL-1β*, *TNF-α*, and *IL-18* mRNA and contents were increased in BV-2 cells subjected to OGD/R, while this increase was alleviated by the inhibition of *Vav1* (**Figure 7A** and **B**). Furthermore, more NLRP3-positive cells were seen in the OGD/R cells compared with the control cells (**Figure 7C** and **D**), while *Vav1* inhibition reversed this effect. Similar to the *in vivo* results, silencing *Vav1* reversed the changes in NLRP3, ASC, and cleaved caspase-1 (p20) levels observed in BV-2 cells subjected to OGD/R (**Figure 7E** and **F**). These findings confirm that *Vav1* knockdown represses inflammation *in vitro*.

Discussion

Several studies have demonstrated that cerebral ischemia is strongly related to inflammation, oxidative stress, and apoptosis (Li et al., 2019b; Gao et al., 2022). Given that the neuronal injury caused by cerebral I/R is irreversible, patients with cerebral ischemia usually have a poor prognosis (Li et al., 2020). Accordingly, blocking inflammation and apoptosis may help reduce the effects of cerebral I/R injury. In this study, we found that *Vav1* was upregulated in MCAO/R rats and in BV-2 cells subjected to OGD/R. Inhibition of *Vav1* suppressed the activation of microglial and NLRP3 inflammasome and decreased the expression of apoptotic regulators, thus alleviating the inflammation and neuronal apoptosis caused by cerebral I/R.

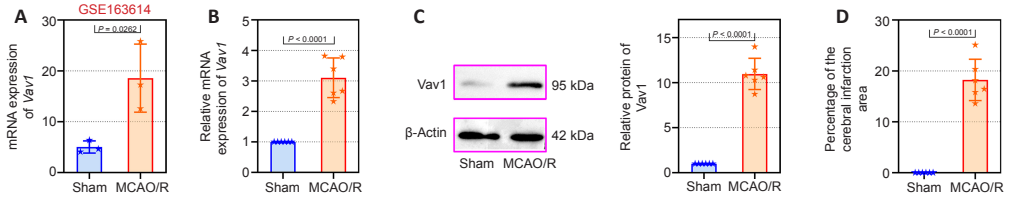

Figure 1 | **Increased *Vav1* expression in the ischemic penumbra of MCAO/R rats.**
(A) *Vav1* mRNA expression in MCAO/R rats according to the GEO database GSE163614. (B) *Vav1* mRNA expression (normalized to the sham group) in the ischemic penumbra of MCAO/R rats. (C) Normalized Vav1 protein expression in the ischemic penumbra of MCAO/R rats. (D) Cerebral infarction area expressed as a percentage of total brain area, as determined by TTC staining. Data are expressed as the mean ± SD (n = 6), and were analyzed by unpaired t-test. The experiments were repeated three times. GEO: Gene expression omnibus; MCAO/R: middle cerebral artery occlusion/reperfusion; TTC staining: triphenyltetrazolium chloride staining; Vav1: Vav guanine nucleotide exchange factor 1.

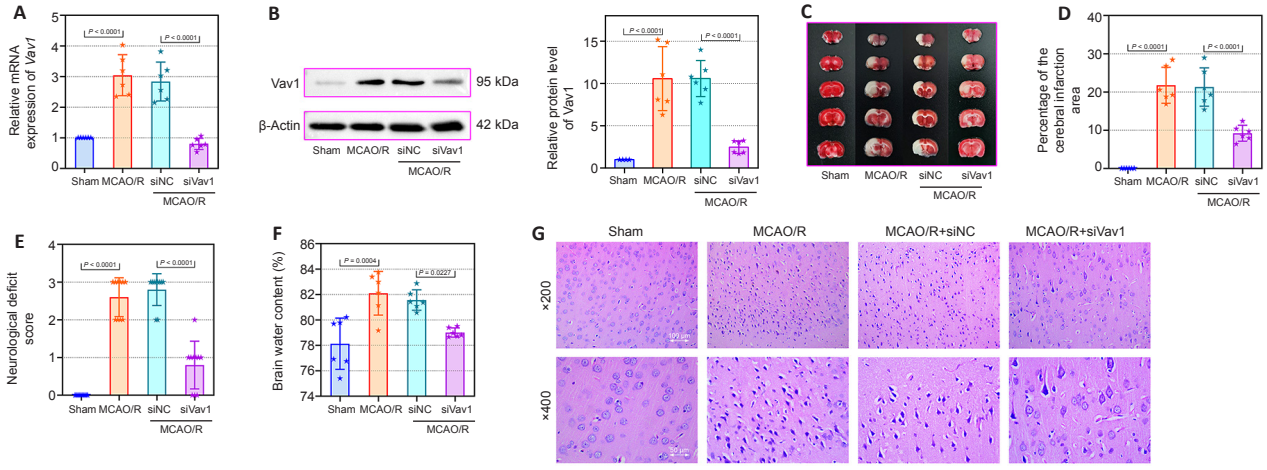

Figure 2 | ***Vav1* knockdown decreases brain infarction area and neuronal injury in MCAO/R rats.**
(A) *Vav1* mRNA expression (normalized to the sham group) in MCAO/R rats, as detected by qPCR. (B) Vav1 protein expression (normalized to the sham group) in MCAO/R rats, as detected by western blot. (C) TTC staining images of cerebral infarction area in MCAO/R rat brain tissues. MCAO/R rats showed increased infarction area compared with sham rats, while Vav1 knockdown reversed this effect. The white area represents the infarction area. (D) Quantitation of the cerebral infarction results. (E) Neurological deficiency scores of MCAO/R rats. (F) Brain water content of MCAO/R rats. (G) Hematoxylin and eosin staining of the cerebral infarction area in MCAO/R rats. The MCAO/R rats showed more damage in the ischemic penumbra than sham rats, but inhibition of Vav1 expression reversed this effect. Scale bars: 100 μm (upper) and 50 μm (lower). Data are expressed as the mean ± SD (n = 10 (E), n = 6 (others)), and were analyzed by one-way analysis of variance followed by Tukey's multiple comparisons test. The experiments were repeated three times. MCAO/R: Middle cerebral artery occlusion/reperfusion; qPCR: quantitative polymerase chain reaction; TTC staining: triphenyltetrazolium chloride staining; Vav1: Vav guanine nucleotide exchange factor 1.

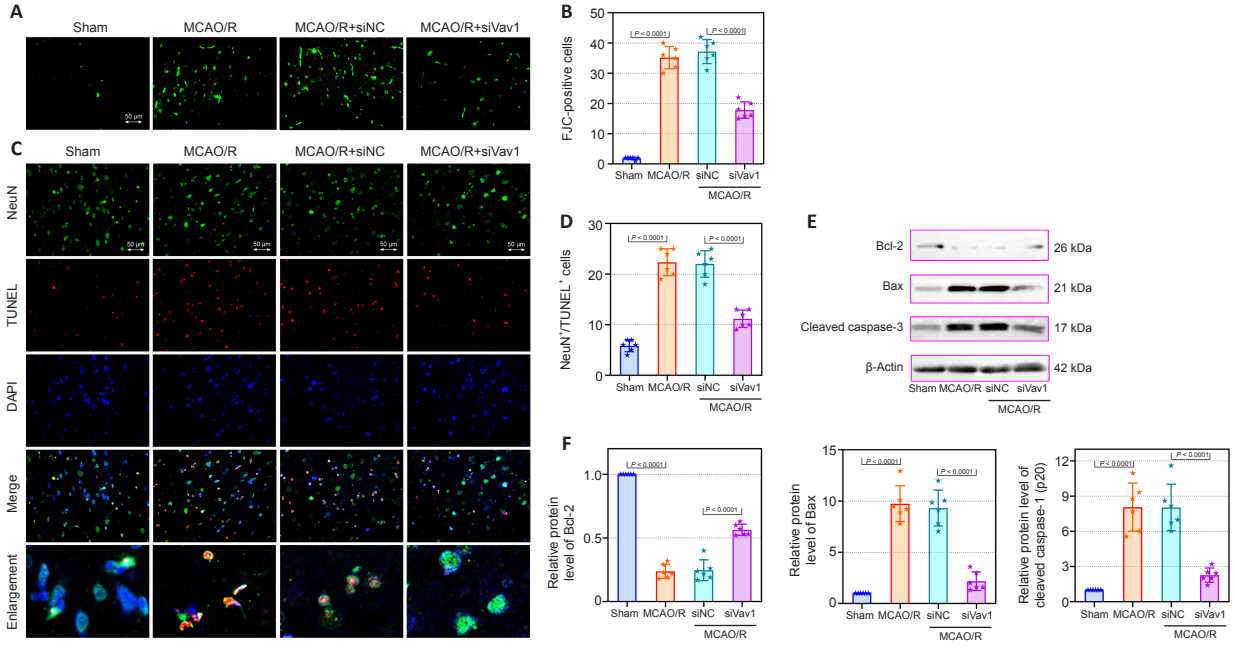

Figure 3 | ***Vav1* knockdown alleviates neuronal loss and apoptosis in the ischemic penumbra of MCAO/R rats.**
(A) FJC staining of the ischemic penumbra area of brain tissues in MCAO/R rats. (B) Quantification of FJC-positive cells (green). (C) Immunofluorescence staining of neurons (NeuN, FITC, green) and TUNEL (red) staining in the ischemic penumbra area in MCAO/R rats. MCAO/R rats showed greater number of TUNEL-positive cells than sham rats, but inhibition of Vav1 decreased this effect. Nuclei were stained with DAPI (blue). Scale bars: 50 μm. (D) Quantification of NeuN and TUNEL double positive cells. (E, F) Bcl-2, Bax, and cleaved caspase-3 protein levels (normalized to the sham group) were analyzed by western blot. Data are expressed as the mean ± SD (n = 6), and were analyzed by one-way analysis of variance followed by Tukey's multiple comparisons test. The experiments were repeated three times. DAPI: 4′,6-Diamidino-2-phenylindole; FITC: fluorescein isothiocyanate; FJC staining: Fluoro-Jade C staining; MCAO/R: middle cerebral artery occlusion/reperfusion; NeuN: neuronal nuclear; TUNEL: terminal-deoxynucleotidyl transferase mediated nick end labeling; Vav1: Vav guanine nucleotide exchange factor 1.

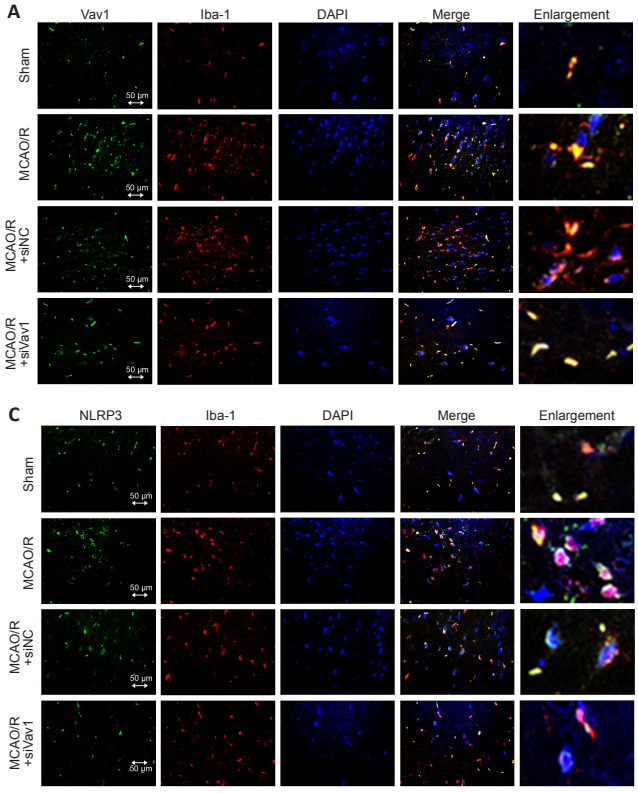

Figure 4 | *Vav1* knockdown represses the activation of microglia and NLRP3 inflammasome in the ischemic penumbra of MCAO/R rats.
(A) Double immunofluorescence staining for Vav1 (FITC, green) and Iba-1 (Cy3, red) in the ischemic penumbra area in MCAO/R rats. MCAO/R rats showed enhanced expression of Vav1 and Iba-1 compared with the sham group, but inhibition of Vav1 expression decreased the levels of both proteins. (B) Quantification of Vav1/Iba-1 double positive cells. (C) Double immunofluorescence staining for NLRP3 (FITC, green) and Iba-1 (Cy3, red) in the ischemic penumbra area in MCAO/R rats. MCAO/R rats showed enhanced expression of Iba-1 and NLRP3 compared with the sham group, but inhibition of Vav1 expression decreased the levels of both proteins. Nuclei were stained with DAPI (blue). Scale bars: 50 μm. (D) Quantification of NLRP3 and Iba-1 double positive cells. Data are expressed as the mean ± SD (n = 6), and were analyzed by one-way analysis of variance followed by Tukey's multiple comparisons test. Cy3: Cyanine 3; DAPI: 4′,6-diamidino-2-phenylindole; FITC: fluorescein isothiocyanate; MCAO/R: middle cerebral artery occlusion/reperfusion; NLRP3: NOD-like receptor pyrin 3; Vav1: Vav guanine nucleotide exchange factor 1.

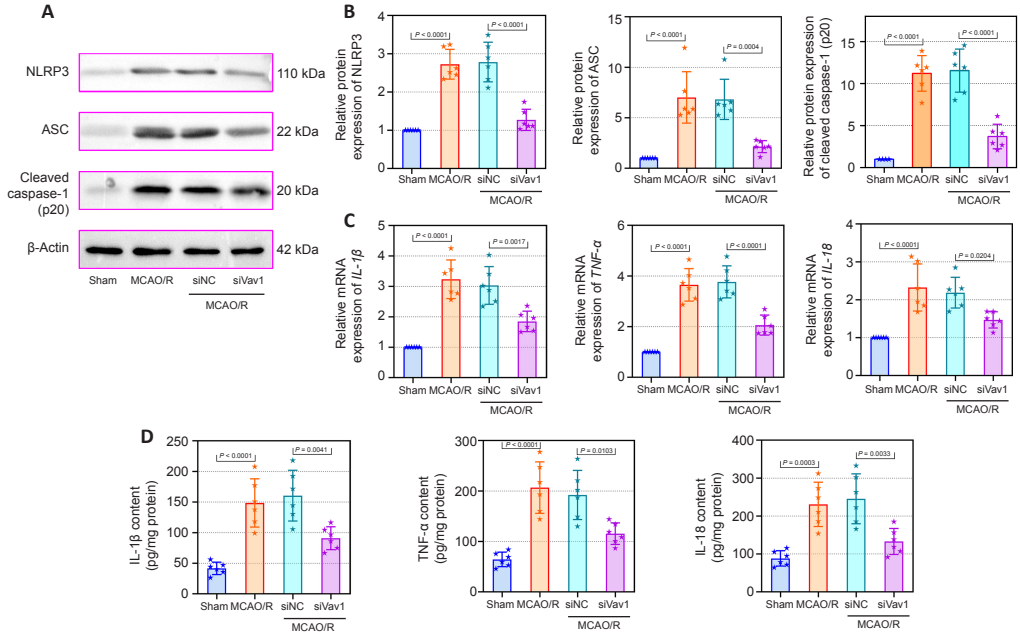

Figure 5 | *Vav1* knockdown represses inflammation in the ischemic penumbra of MCAO/R rats.
(A, B) NLRP3, ASC, and cleaved caspase-1 (p20) expression levels in the ischemic penumbra area in MCAO/R rats (normalized to the sham group) were analyzed by western blot. (C) *IL-1β*, *TNF-α*, and *IL-18* mRNA expression levels (normalized to the sham group) in the ischemic penumbra area of MCAO/R rats were analyzed by qPCR. (D) The contents of IL-1β, TNF-α, and IL-18 in the ischemic penumbra area of MCAO/R rats were analyzed by ELISA. Data are expressed as the mean ± SD (n = 6), and were analyzed by one-way analysis of variance followed by Tukey's multiple comparisons test. The experiments were repeated three times. ASC: Apoptosis-associated speck-like protein; ELISA: enzyme-linked immunosorbent assay; IL-18: interleukin-18; IL-1β: interleukin-1β; MCAO/R: middle cerebral artery occlusion/reperfusion; NLRP3: NOD-like receptor pyrin 3; qPCR: quantitative polymerase chain reaction; TNF-α: tumor necrosis factor-α; Vav1: Vav guanine nucleotide exchange factor 1.

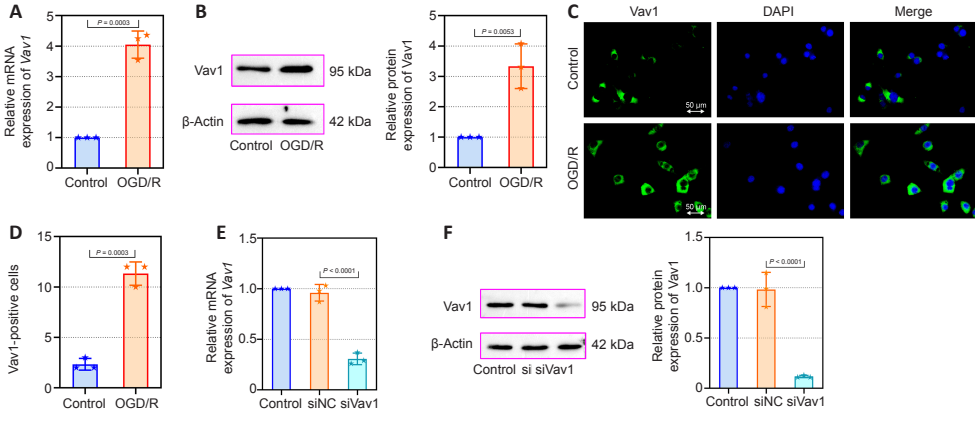

Figure 6 | Increased *Vav1* expression in BV-2 cells subjected to OGD/R.
(A) *Vav1* mRNA expression in control BV-2 cells and BV-2 cells subjected to OGD/R. (B) Vav1 protein expression in control BV-2 cells and BV-2 cells subjected to OGD/R. (C) Immunofluorescence staining for Vav1 in control BV-2 cells and BV-2 cells subjected to OGD/R. Compared with the control cells, Vav1 expression was increased in OGD/R cells. Nuclei were stained with DAPI (blue). Scale bars: 50 μm. (D) Quantification of Vav1-positive cells. (E) *Vav1* mRNA expression in *Vav1* knockdown BV-2 cells. (F) Vav1 protein expression in *Vav1* knockdown BV-2 cells. Data are expressed as the mean ± SD, and were analyzed by unpaired t-test (A, B, D) or one-way analysis of variance followed by Tukey's multiple comparisons test (E, F). The experiments were repeated three times. DAPI: 4′,6-Diamidino-2-phenylindole; OGD/R: oxygen-glucose deprivation/reoxygenation; Vav1: Vav guanine nucleotide exchange factor 1.

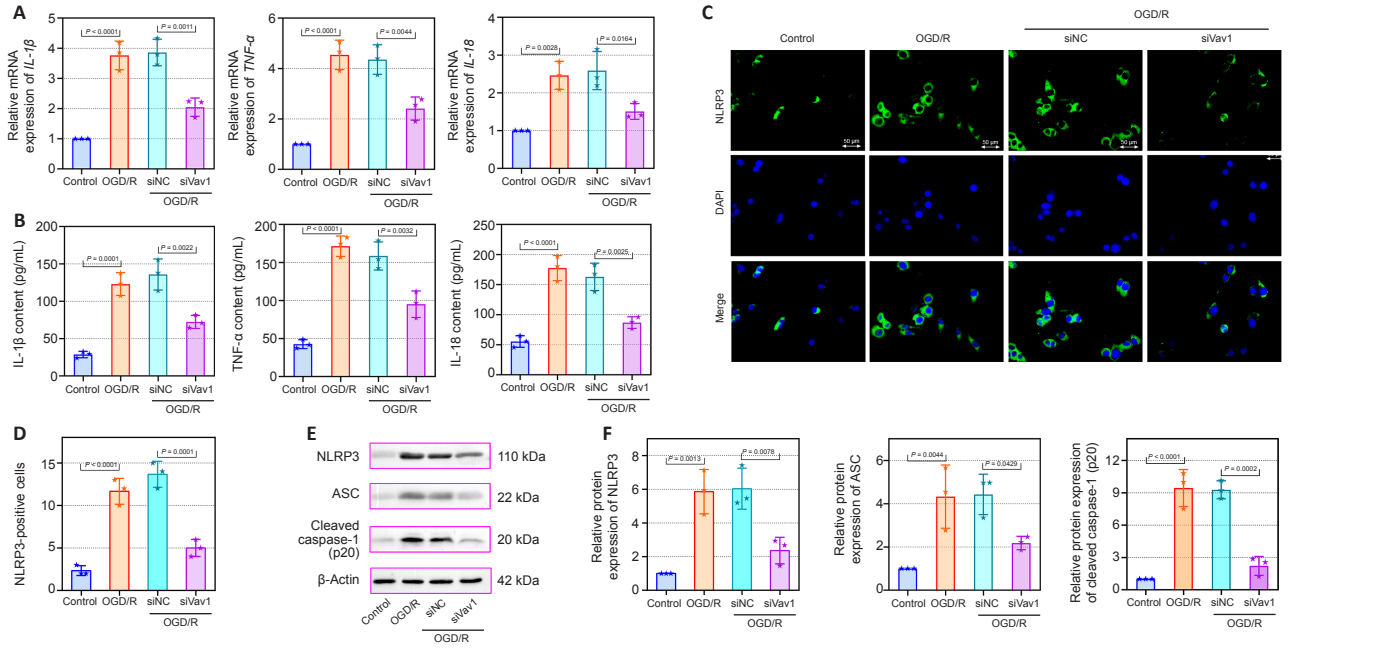

Figure 7 | ***Vav1* knockdown represses inflammation in BV-2 cells subjected to OGD/R.**
(A) *IL-1β*, *TNF-α*, and *IL-18* mRNA levels in control BV-2 cells and BV-2 cells subjected to OGD/R were analyzed by qPCR. (B) The contents of IL-1β, TNF-α, and IL-18 in control BV-2 cells and BV-2 cells subjected to OGD/R were detected by ELISA. (C) Immunofluorescence staining for NLRP3 (FITC, green) in BV-2 cells subjected to OGD/R. Compared with control cells, NLRP3 expression was increased in BV-2 cells subjected to OGD/R, while inhibition of Vav1 expression decreased NLRP3 expression. Nuclei were stained with DAPI (blue). Scale bars: 50 μm. (D) Quantification of NLRP3 positive cells. (E, F) NLRP3, ASC, and cleaved caspase-1 (p20) protein levels in BV-2 cells subjected to OGD/R were analyzed by western blot. Data are expressed as the mean ± SD, and were analyzed by one-way analysis of variance followed by Tukey's multiple comparisons test. The experiments were repeated three times. ASC: Apoptosis-associated speck-like protein; DAPI: 4′,6-diamidino-2-phenylindole; ELISA: enzyme-linked immunosorbent assay; FITC: fluorescein isothiocyanate; IL-18: interleukin-18; IL-1β: interleukin-1β; NLRP3: NOD-like receptor pyrin 3; OGD/R: oxygen-glucose deprivation/reoxygenation; qPCR: quantitative polymerase chain reaction; TNF-α: tumor necrosis factor-α; Vav1: Vav guanine nucleotide exchange factor 1.

In this study, we used male rats as the *in vivo* study subject. First, studies show that, in brain injury, higher levels of infarction and disability are found in male than in female individuals (El-Hakim et al., 2021), which may due to the protective effect of the female sex hormones estrogen and progesterone (Vahidinia et al., 2021). Therefore, to avoid the influence of these hormones, male mice were selected for our experiments. More importantly, in this work, we found that *Vav1* is related to microglial activation. Studies have found that the increase in resident microglia proliferation in the injured cerebral hemisphere is higher in male rats compared to female rats. Furthermore, Iba-staining for microglia is greater in male than in female rats after brain injury, indicating a greater number of microglia (Scott et al., 2022). The GSE163614 database and our *in vivo* model both demonstrate that *Vav1* is highly expressed in MCAO/R rats. To further explore the role of elevated *Vav1* levels in MCAO/R rats, we examined the effect of *Vav1* on neurological impairment after cerebral I/R. The results showed that inhibition of *Vav1* expression decreased infarction area, neurological deficit, brain water content, and cerebral tissue damage in MCAO/R rats. These findings demonstrate that inhibiting *Vav1* expression moderates the deleterious effects of I/R, indicating that *Vav1* plays an essential role in cerebral I/R injury. On the basis of this, we explored the potential mechanism of *Vav1* regulation in cerebral I/R injury. *Vav1* has been reported to be related to neuronal apoptosis (He et al., 2020) and microglial activation (Chen et al., 2017) in other neurodegenerative diseases. Accordingly, we hypothesized that *Vav1* may be closely related to the activation of microglial and NLRP3 inflammasome activation, thus playing a key role in cerebral I/R injury.

Cerebral I/R can induce cell death (Gong et al., 2017), and cell apoptosis is considered to play an essential part in cerebral I/R injury (Bredesen et al., 2006; Hausburg et al., 2020). In our study, we explored the role of *Vav1* in neuronal apoptosis. Given that Bcl-2 and Bax are closely involved in apoptosis (Li et al., 2018), we examined changes in the expression levels of these two proteins. Silencing *Vav1* clearly decreased neuronal apoptosis in MCAO/R rats, as revealed by the decreased levels of cleaved caspase-3 and Bcl2, and the increased level of Bax.

In addition to apoptosis, inflammation following cerebral ischemia is a risk factor for cerebral I/R injury. Among the factors associated with cerebral ischemic inflammation, *IL-1β*, *IL-18*, and *TNF-α* show a strong connection with brain injury (Enzmann et al., 2018). Early inflammatory injury after cerebral I/R has been reported to be mainly caused by the pro-inflammatory mediator *TNF-α*, and its release is closely related to activated microglia (Tuttolomondo et al., 2009). In addition, one study showed that microglia activate the NLRP3 inflammasome, thereby promoting inflammation, and that silencing NLRP3 expression reduced levels of pro-inflammatory cytokines, thereby inhibiting neuroinflammation and reducing tissue damage (Yang et al., 2014). Considering the important role of microglia in cerebral I/R injury, we measured the expression level of Iba1, a microglial marker, in MCAO/R rats. The results showed an increase in Iba-1 expression after cerebral I/R. More importantly, we found that *Vav1* and NLRP3 were localized almost exclusively to Iba-1-positive cells, and *Vav1* inhibition reversed the increase in Iba-1 and NLRP3 expression in MCAO/R rats. This phenomenon reflected the result that MCAO/R induced high levels of *Vav1* expression in microglia, and *Vav1* inhibition decreased microglial and NLRP3 inflammasome activation.

A previous study found that *Vav1* expression is related to LPS-induced microglial activation (Chen et al., 2017). Under ischemic conditions, the NLRP3 inflammasome is activated, and the expression levels of its core proteins, including NLRP3, ASC, caspase-1, IL-1, and IL-18, increases (Fann et al., 2013). Similarly, we found substantially increased NLRP3, ASC, and cleaved caspase-1 (p20) levels in MCAO/R rats, while inhibition of *Vav1* reversed this effect. Previous studies have shown that inhibiting NLRP3 inflammasome activation reduces inflammation, infarct size, and edema formation (Yang et al., 2014; Dong et al., 2016). Therefore, we measured the expression levels of TNF-α, IL-1β, and IL-18, which are downstream effectors of activated microglia and NLRP3. *Vav1* knockdown has been reported to reduce LPS-induced production of TNF-α by macrophages (Miletic et al., 2007). Consistent with this, we found that *Vav1* inhibition significantly decreased cerebral I/R-induced elevation of pro-inflammatory factor expression. Therefore, we inferred that *Vav1* may be involved in cerebral I/R injury by affecting the activation of microglial and NLRP3 inflammasome. To confirm the role of *Vav1 in vitro*, we constructed an OGD/R cell model in BV-2 microglia cells. Consistent with the *in vivo* results, *Vav1* was upregulated in BV-2 cells subjected to OGD/R. Inhibiting *Vav1* decreased NLRP3 inflammasome activation and the release of pro-inflammatory factors in BV-2 cells.

Overall, we found that *Vav1* plays a significant role in cerebral I/R injury. In this study, we chose to inhibit *Vav1* expression before surgery. Although this method is commonly used in studies that explore the functional role that genes play in cerebral I/R injury (Li et al., 2019a; Wang et al., 2020b; Chen et al., 2021; Han et al., 2021), it was still a limitation of our current research. Because the role of *Vav1* in MCAO/R has not been previously reported, our current study presents only preliminary results demonstrating that *Vav1* inhibition decreases the level of brain injury caused by MCAO/R. Further research is needed to provide a basis for potential drug development and other clinical applications based on our results.

In this study, we found that *Vav1* is highly expressed in MCAO/R rats. *Vav1* inhibition reduced the inflammation and neuronal apoptosis seen in MCAO/R rats by inhibiting the activation of microglial and NLRP3 inflammasome.

Author contributions: *Conceptualization and manuscript original draft: JQ, JG; investigation: JQ, XS; methodology: JG, XS; data curation and formal analysis: LL, XL; manuscript review & editing: JQ, JG, HC; funding acquisition: JQ. All authors approved the final version of the manuscript.*
Conflicts of interest: *The authors have no conflict of interest to declare.*
Data availability statement: *The data are available from the corresponding author on reasonable request.*

Open peer reviewers: *Vanessa Castelli, University of L'Aquila, Italy; Huerta de la Cruz, University of Vermont, USA.*

Additional file: *Open peer review reports 1 and 2.*

References

Bavarsad K, Barreto GE, Hadjzadeh MA, Sahebkar A (2019) Protective effects of curcumin against ischemia-reperfusion injury in the nervous system. Mol Neurobiol 56:1391-1404.
Bredesen DE, Rao RV, Mehlen P (2006) Cell death in the nervous system. Nature 443:796-802.
Campbell BCV, De Silva DA, Macleod MR, Coutts SB, Schwamm LH, Davis SM, Donnan GA (2019) Ischaemic stroke. Nat Rev Dis Primers 5:70.
Chandra A, Stone CR, Du X, Li WA, Huber M, Bremer R, Geng X, Ding Y (2017) The cerebral circulation and cerebrovascular disease III: Stroke. Brain Circ 3:66-77.
Chen XY, Wan SF, Yao NN, Lin ZJ, Mao YG, Yu XH, Wang YZ (2021) Inhibition of the immunoproteasome LMP2 ameliorates ischemia/hypoxia-induced blood-brain barrier injury through the Wnt/β-catenin signalling pathway. Mil Med Res 8:62.
Chen Y, Jin Y, Zhan H, Chen J, Chen Y, Meng H, Jin J, Yu L, Cao X, Xu Y (2017) Proteomic analysis of the effects of Nur77 on lipopolysaccharide-induced microglial activation. Neurosci Lett 659:33-43.
Dong Y, Fan C, Hu W, Jiang S, Ma Z, Yan X, Deng C, Di S, Xin Z, Wu G, Yang Y, Reiter RJ, Liang G (2016) Melatonin attenuated early brain injury induced by subarachnoid hemorrhage via regulating NLRP3 inflammasome and apoptosis signaling. J Pineal Res 60:253-262.
El-Hakim Y, Mani KK, Eldouh A, Pandey S, Grimaldo MT, Dabney A, Pilla R, Sohrabji F (2021) Sex differences in stroke outcome correspond to rapid and severe changes in gut permeability in adult Sprague-Dawley rats. Biol Sex Differ 12:14.
Enzmann G, Kargaran S, Engelhardt B (2018) Ischemia-reperfusion injury in stroke: impact of the brain barriers and brain immune privilege on neutrophil function. Ther Adv Neurol Disord 11:1756286418794184.
Fann DY, Lee SY, Manzanero S, Tang SC, Gelderblom M, Chunduri P, Bernreuther C, Glatzel M, Cheng YL, Thundyil J, Widiapradja A, Lok KZ, Foo SL, Wang YC, Li YI, Drummond GR, Basta M, Magnus T, Jo DG, Mattson MP, et al. (2013) Intravenous immunoglobulin suppresses NLRP1 and NLRP3 inflammasome-mediated neuronal death in ischemic stroke. Cell Death Dis 4:e790.
Gao Y, Hu M, Niu X, Li M, Xu L, Xiao Y, Zhang J, Wang H, Li L, Chu B, Lv P (2022) Dl-3-n-butylphthalide improves neuroinflammation in mice with repeated cerebral ischemia-reperfusion injury through the Nrf2-mediated antioxidant response and TLR4/MyD88/NF-κB signaling pathway. Oxid Med Cell Longev 2022:8652741.
Gong L, Tang Y, An R, Lin M, Chen L, Du J (2017) RTN1-C mediates cerebral ischemia/reperfusion injury via ER stress and mitochondria-associated apoptosis pathways. Cell Death Dis 8:e3080.
Han B, Jiang W, Cui P, Zheng K, Dang C, Wang J, Li H, Chen L, Zhang R, Wang QM, Ju Z, Hao J (2021) Microglial PGC-1α protects against ischemic brain injury by suppressing neuroinflammation. Genome Med 13:47.
Hausburg MA, Banton KL, Roman PE, Salgado F, Baek P, Waxman MJ, Tanner A, 2nd, Yoder J, Bar-Or D (2020) Effects of propofol on ischemia-reperfusion and traumatic brain injury. J Crit Care 56:281-287.
He B, Chen W, Zeng J, Tong W, Zheng P (2020) MicroRNA-326 decreases tau phosphorylation and neuron apoptosis through inhibition of the JNK signaling pathway by targeting VAV1 in Alzheimer's disease. J Cell Physiol 235:480-493.
He Q, Wang S, Liu X, Guo H, Yang H, Zhang L, Zhuang P, Zhang Y, Ye Z, Hu L (2015) Salvianolate lyophilized injection promotes post-stroke functional recovery via the activation of VEGF and BDNF-TrkB-CREB signaling pathway. Int J Clin Exp Med 8:108-122.
Henske EP, Short MP, Jozwiak S, Bovey CM, Ramlakhan S, Haines JL, Kwiatkowski DJ (1995) Identification of VAV2 on 9q34 and its exclusion as the tuberous sclerosis gene TSC1. Ann Hum Genet 59:25-37.
Hong J, Min Y, Wuest T, Lin PC (2020) Vav1 is essential for HIF-1α activation via a lysosomal VEGFR1-mediated degradation mechanism in endothelial cells. Cancers (Basel) 12:1374.
Inoue M, Williams KL, Oliver T, Vandenabeele P, Rajan JV, Miao EA, Shinohara ML (2012) Interferon-β therapy against EAE is effective only when development of the disease depends on the NLRP3 inflammasome. Sci Signal 5:ra38.
Ji J, Xiang P, Li T, Lan L, Xu X, Lu G, Ji H, Zhang Y, Li Y (2017) NOSH-NBP, a novel nitric oxide and hydrogen sulfide- releasing hybrid, attenuates ischemic stroke-induced neuroinflammatory injury by modulating microglia polarization. Front Cell Neurosci 11:154.
Kalogeris T, Baines CP, Krenz M, Korthuis RJ (2012) Cell biology of ischemia/reperfusion injury. Int Rev Cell Mol Biol 298:229-317.
Katzav S, Martin-Zanca D, Barbacid M (1989) vav, a novel human oncogene derived from a locus ubiquitously expressed in hematopoietic cells. EMBO J 8:2283-2290.
Kim SR, Park HJ, Lee KB, Kim HJ, Jeong JS, Cho SH, Lee YC (2020) Epithelial PI3K-δ promotes house dust mite-induced allergic asthma in NLRP3 inflammasome-dependent and -independent manners. Allergy Asthma Immunol Res 12:338-358.
Lambertsen KL, Biber K, Finsen B (2012) Inflammatory cytokines in experimental and human stroke. J Cereb Blood Flow Metab 32:1677-1698.
Lavezzi AM, Corna MF, Matturri L (2013) Neuronal nuclear antigen (NeuN): a useful marker of neuronal immaturity in sudden unexplained perinatal death. J Neurol Sci 329:45-50.
Li C, Tang B, Feng Y, Tang F, Pui-Man Hoi M, Su Z, Ming-Yuen Lee S (2018) Pinostrobin exerts neuroprotective actions in neurotoxin-induced Parkinson's disease models through Nrf2 induction. J Agric Food Chem 66:8307-8318.
Li F, Xu Y, Li X, Wang X, Yang Z, Li W, Cheng W, Yan G (2021) Triblock copolymer nanomicelles loaded with curcumin attenuates inflammation via inhibiting the NF-κB pathway in the rat model of cerebral ischemia. Int J Nanomedicine 16:3173-3183.
Li J, Zhang J, Zhang Y, Wang Z, Song Y, Wei S, He M, You S, Jia J, Cheng J (2019a) TRAF2 protects against cerebral ischemia-induced brain injury by suppressing necroptosis. Cell Death Dis 10:328.
Li TF, Ma J, Han XW, Jia YX, Yuan HF, Shui SF, Guo D, Yan L (2019b) Chrysin ameliorates cerebral ischemia/reperfusion (I/R) injury in rats by regulating the PI3K/Akt/mTOR pathway. Neurochem Int 129:104496.
Li TT, Wan Q, Zhang X, Xiao Y, Sun LY, Zhang YR, Liu XN, Yang WC (2022) Stellate ganglion block reduces inflammation and improves neurological function in diabetic rats during ischemic stroke. Neural Regen Res 17:1991-1997.
Li Y, Li S, Li D (2020) Breviscapine alleviates cognitive impairments induced by transient cerebral ischemia/reperfusion through its anti-inflammatory and anti-oxidant properties in a rat model. ACS Chem Neurosci 11:4489-4498.
Liang HW, Qiu SF, Shen J, Sun LN, Wang JY, Bruce IC, Xia Q (2008) Genistein attenuates oxidative stress and neuronal damage following transient global cerebral ischemia in rat hippocampus. Neurosci Lett 438:116-120.
Livak KJ, Schmittgen TD (2001) Analysis of relative gene expression data using real-time quantitative PCR and the 2(-Delta Delta C(T)) Method. Methods 25:402-408.
Longa EZ, Weinstein PR, Carlson S, Cummins R (1989) Reversible middle cerebral artery occlusion without craniectomy in rats. Stroke 20:84-91.
Marlier Q, Verteneuil S, Vandenbosch R, Malgrange B (2015) Mechanisms and functional significance of stroke-induced neurogenesis. Front Neurosci 9:458.
Miletic AV, Graham DB, Montgrain V, Fujikawa K, Kloeppel T, Brim K, Weaver B, Schreiber R, Xavier R, Swat W (2007) Vav proteins control MyD88-dependent oxidative burst. Blood 109:3360-3368.
Moskowitz MA, Lo EH, Iadecola C (2010) The science of stroke: mechanisms in search of treatments. Neuron 67:181-198.
Movilla N, Bustelo XR (1999) Biological and regulatory properties of Vav-3, a new member of the Vav family of oncoproteins. Mol Cell Biol 19:7870-7885.
Øie LR, Kurth T, Gulati S, Dodick DW (2020) Migraine and risk of stroke. J Neurol Neurosurg Psychiatry 91:593-604.
Percie du Sert N, Hurst V, Ahluwalia A, Alam S, Avey MT, Baker M, Browne WJ, Clark A, Cuthill IC, Dirnagl U, Emerson M, Garner P, Holgate ST, Howells DW, Karp NA, Lazic SE, Lidster K, MacCallum CJ, Macleod M, Pearl EJ, et al. (2020) The ARRIVE guidelines 2.0: Updated guidelines for reporting animal research. PLoS Biol 18:e3000410.
Scott MC, Prabhakara KS, Walters AJ, Olson SD, Cox CS, Jr. (2022) Determining sex-based differences in inflammatory response in an experimental traumatic brain injury model. Front Immunol 13:753570.
Shah VB, Ozment-Skelton TR, Williams DL, Keshvara L (2009) Vav1 and PI3K are required for phagocytosis of beta-glucan and subsequent superoxide generation by microglia. Mol Immunol 46:1845-1853.
Stegner D, Klaus V, Nieswandt B (2019) Platelets as modulators of cerebral ischemia/reperfusion injury. Front Immunol 10:2505.
Sun X, Wang D, Zhang T, Lu X, Duan F, Ju L, Zhuang X, Jiang X (2020) Eugenol attenuates cerebral ischemia-reperfusion injury by enhancing autophagy via AMPK-mTOR-P70S6K pathway. Front Pharmacol 11:84.
Sun Y, Jin K, Xie L, Childs J, Mao XO, Logvinova A, Greenberg DA (2003) VEGF-induced neuroprotection, neurogenesis, and angiogenesis after focal cerebral ischemia. J Clin Invest 111:1843-1851.
Surinkaew P, Sawaddiruk P, Apaijai N, Chattipakorn N, Chattipakorn SC (2018) Role of microglia under cardiac and cerebral ischemia/reperfusion (I/R) injury. Metab Brain Dis 33:1019-1030.
Takeda H, Yamaguchi T, Yano H, Tanaka J (2021) Microglial metabolic disturbances and neuroinflammation in cerebral infarction. J Pharmacol Sci 145:130-139.
Tan LL, Jiang XL, Xu LX, Li G, Feng CX, Ding X, Sun B, Qin ZH, Zhang ZB, Feng X, Li M (2021) TP53-induced glycolysis and apoptosis regulator alleviates hypoxia/ischemia-induced microglial pyroptosis and ischemic brain damage. Neural Regen Res 16:1037-1043.
Turner M, Billadeau DD (2002) VAV proteins as signal integrators for multi-subunit immune-recognition receptors. Nat Rev Immunol 2:476-486.
Tuttolomondo A, Di Sciacca R, Di Raimondo D, Renda C, Pinto A, Licata G (2009) Inflammation as a therapeutic target in acute ischemic stroke treatment. Curr Top Med Chem 9:1240-1260.
Vahidinia Z, Mahdavi E, Talaei SA, Naderian H, Tamtaji A, Haddad Kashani H, Beyer C, Azami Tameh A (2021) The effect of female sex hormones on Hsp27 phosphorylation and histological changes in prefrontal cortex after tMCAO. Pathol Res Pract 221:153415.
Wang F, Li R, Tu P, Chen J, Zeng K, Jiang Y (2020a) Total glycosides of cistanche deserticola promote neurological function recovery by inducing neurovascular regeneration via Nrf-2/Keap-1 pathway in MCAO/R rats. Front Pharmacol 11:236.
Wang H, Zheng X, Jin J, Zheng L, Guan T, Huo Y, Xie S, Wu Y, Chen W (2020b) LncRNA MALAT1 silencing protects against cerebral ischemia-reperfusion injury through miR-145 to regulate AQP4. J Biomed Sci 27:40.
Wang M, Pan W, Xu Y, Zhang J, Wan J, Jiang H (2022) Microglia-mediated neuroinflammation: a potential target for the treatment of cardiovascular diseases. J Inflamm Res 15:3083-3094.
Wang T, Zhao N, Peng L, Li Y, Huang X, Zhu J, Chen Y, Yu S, Zhao Y (2020c) DJ-1 regulates microglial polarization through P62-mediated TRAF6/IRF5 signaling in cerebral ischemia-reperfusion. Front Cell Dev Biol 8:593890.
Wu XJ, Sun XH, Wang SW, Chen JL, Bi YH, Jiang DX (2018) Mifepristone alleviates cerebral ischemia-reperfusion injury in rats by stimulating PPAR γ. Eur Rev Med Pharmacol Sci 22:5688-5696.
Xu J, Zhang QG, Li C, Zhang GY (2007) Subtoxic N-methyl-D-aspartate delayed neuronal death in ischemic brain injury through TrkB receptor- and calmodulin-mediated PI-3K/Akt pathway activation. Hippocampus 17:525-537.
Yang F, Wang Z, Wei X, Han H, Meng X, Zhang Y, Shi W, Li F, Xin T, Pang Q, Yi F (2014) NLRP3 deficiency ameliorates neurovascular damage in experimental ischemic stroke. J Cereb Blood Flow Metab 34:660-667.
Yi D, Wang Q, Zhao Y, Song Y, You H, Wang J, Liu R, Shi Z, Chen X, Luo Q (2021) Alteration of N (6)-methyladenosine mRNA methylation in a rat model of cerebral ischemia-reperfusion injury. Front Neurosci 15:605654.
Zangiabadi S, Abdul-Sater AA (2022) Regulation of the NLRP3 inflammasome by posttranslational modifications. J Immunol 208:286-292.
Zeng X, Zhang YD, Ma RY, Chen YJ, Xiang XM, Hou DY, Li XH, Huang H, Li T, Duan CY (2022) Activated Drp1 regulates p62-mediated autophagic flux and aggravates inflammation in cerebral ischemia-reperfusion via the ROS-RIP1/RIP3-exosome axis. Mil Med Res 9:25.

P-Reviewers: Castelli V, de la Cruz H; C-Editor: Zhao M; S-Editors: Yu J, Li CH; L-Editors: Crow E, Yu J, Song LP; T-Editor: Jia Y